GPX7 is Identified as a Novel Prognostic Indicator for Brain Lower Grade Glioma (LGG): Evidence from a Pan-Cancer Analysis

Qianqian Zhao
School of Nursing,Shaanxi University of Chinese Medicine
Yin Yang
The Second Department of Orthopedics, Xi'an Central Hospital
Luyu Zhang
School of Nursing,Shaanxi University of Chinese Medicine
Yingying Wang
School of Nursing,Shaanxi University of Chinese Medicine
Tianpei Wang
School of Nursing,Shaanxi University of Chinese Medicine
Ye Sun
School of Nursing,Shaanxi University of Chinese Medicine
Jingjing Cao
School of Nursing,Shaanxi University of Chinese Medicine
Meng Qi
Ankang R&D Center of Se-enriched Products,Shaanxi
Xiaoping Du
Ankang R&D Center of Se-enriched Products,Shaanxi
Zengrun Xia
Ankang R&D Center of Se-enriched Products,Shaanxi
Rongqiang Zhang (✉ Zhangrqxianyang@163.com)
School of Public Health,Shaanxi University of Chinese Medicine

Research Article

Keywords: GPX7, pan-cancer, gene expression, prognosis, Brain Lower Grade Glioma

Posted Date: August 26th, 2021

DOI: https://doi.org/10.21203/rs.3.rs-763552/v1

Abstract

Background: Glutathione peroxidase-7 (*GPX7*), a newly discovered non-selenium-containing protein with glutathione peroxidase activity, is located near the endoplasmic reticulum. Various studies have reported the involvement of *GPX7* in cancer disease progression. However, the expression patterns of *GPX7* and its prognostic potential have not been evaluated from a pan-cancer perspective. Moreover, the relationship between *GPX7* and prognosis in Brain Lower Grade Glioma (LGG) patients remains unclear.

Methods: Expression levels of *GPX7* were evaluated using the Cancer Genome Atlas (TCGA) and the Genotype-Tissue Expression (GTEx) databases. Kaplan-Meier plotter and Gene Expression Profiling Interactive Analysis (GEPIA2) were used to evaluate the effect of *GPX7* on clinical prognosis in TCGA tumors. Correlations between *GPX7* and cancer immune infiltrates were investigated using the Tumor Immune Estimation Resource (TIMER) site and Estimating the Proportions of Immune and Cancer cells (EPIC) algorithm. In addition, the GEPIA2 and STRING websites were used for enrichment analysis of *GPX7*-related genes. Finally, we constructed a prognostic Nomogram for LGG to verify the overall survival (OS) outcomes of patients.

Results: *GPX7* was found to be overexpressed in multiple tumors. Elevated expression levels of *GPX7* were associated with poor prognosis regarding OS, disease-free survival (DFS) and progression-free survival (PFS) of LGG patients (OS Hazard ratio (HR) = 1.044, $p < 0.0001$; DFS HR = 1.035, $p < 0.0001$; PFS HR = 1.045, $p < 0.0001$). Concordance index (C-index) of the nomogram for LGG was 0.845 (95% CI, 0.825 to 0.865; $p < 0.001$). The nomogram exhibited a better predictability. In addition, *GPX7* expression and the abundance of Cancer-associated fibroblasts (CAFs) were positively correlated in most cancer types. Enrichment analysis revealed that *GPX7* may be involved in the glutathione derivative biosynthetic and glutathione metabolic biological processes.

Conclusion: *GPX7* was found to be upregulated in multiple tumors, which was correlated with poor prognosis in LGG. Therefore, *GPX7* is a potential prognostic indicator for LGG. There is a strong correlation between *GPX7* expression levels and glutathione metabolic pathways. *GPX7* holds promise for the use of glutathione metabolism for guided therapy in cancer patients.

Background

Globally, due to the increasing morbidity and mortality rates, cancer is a major public health concern. According to the World Health Organization (WHO), global cancer cases have been estimated to increase by 60% in the next 20 years, therefore, there is a need to establish better prevention and control indicators [1]. According to the latest data of the latest edition of the Global Cancer Report released by the International Agency for Research on Cancer (IARC) of the WHO in 2020, the number of new global cancers cases are around 19.29 million around [2]. Cancer is associated with a heavy economic and social burden, and seriously threatens human health and safety. It is a complex multi-step disease with extremely complex biological characteristics. Due to different etiologies and complicated pathogenesis of

cancer, the therapeutic options for cancer are quite different. Currently, the main therapeutic options include surgery, chemotherapy, radiotherapy and systemic treatment, which have curative effects. However, cancer therapy is associated with various limitations. Mortality rates for cancer patients are relatively high, and their prognosis is quite poor. Studies are aimed at developing strategies for predicting the prognosis and early diagnosis of cancer, however, there is a lack of effective biomarkers and predictive indicators. Therefore, identification of effective tumor markers is essential for improving the survival rate of cancer patients.

The glutathione peroxidase (*GPXs*) family is an important member of the selenoprotein family. It is one of the important antioxidant enzymes, and an important reactive oxygen species (ROS) free radical scavenger in an organism. There are 8 types of *GPXs*, named *GPX1-GPX8*, of which *GPX1-GPX4* and *GPX6* are *GPXs* containing selenocysteine, while *GPX5, GPX7* and *GPX8* are non-selenocysteine *GPXs* [3–6]. Glutathione peroxidase-7 (*GPX7*) is important in alleviation of the damage associated with ROS to body cells and is also involved in maintaining body redox homeostasis [7]. Studies have shown that the differential expressions of *GPX7* are associated with some tumors, including breast cancer [3], gastric cancer [8], esophageal cancer [9], glioma [10] and hepatocellular carcinoma [11] among others. Although *GPX7* gene expression and its transcription characteristics have been detected in various cancers, studies on *GPX7* expression in cancers are limited by small sample sizes, or are focused on a single or limited number of cancers.

Pan-cancer analysis does not refer to a specific tumor, instead, data from different tumor types and multiple sets of platforms are integrated, analyzed, and interpreted to identify and analyze different genetic changes in malignancies [12]. Studies on pan-cancer analysis is getting more and more attention. Through pan-cancer analysis, similarities and differences between genomes and cell changes for different malignant tumor types can be established. Tumorigenesis mechanisms are extremely complicated. The opened and shared databases, including The Cancer Genome Atlas (TCGA) and the Genotype-Tissue Expression (GTEx) contain functional genomic data sets for different tumors. These databases allow for pan-cancer analysis [12–14]. However, due to large amounts of clinical data, expression patterns of *GPX7* as well as its diagnostic and prognostic potential have not been studied from the pan-cancer perspective.

This study aimed at: i. Investigating changes in *GPX7* mRNA expression levels in human normal tissues; ii. Comparing *GPX7* expression levels in tumor tissues vs. normal tissues; iii. Evaluating the association between *GPX7* expression levels and prognosis, gene mutation, immune infiltration, and enrichment of related cell pathways; iv. For our purposes, the association between *GPX7* and Brain Lower Grade Glioma (LGG) was analyzed using the pan-cancer data in this study. This study elucidates on the nature of *GPX7* expression and its biological mechanism in human cancers.

Results

mRNA expression levels of *GPX7* in normal human tissues and cell lines

Figure 1A shows that *GPX7* mRNA expression levels exhibited a low specificity in normal human tissues. It was found to be distributed in all main tissues of the human body, among which the top three were dendritic cells, placental tissue and blood(T-cells). As is shown in figure 1B, the mRNA expression levels of *GPX7* were widely expressed in all cell lines. These findings show that there is a relatively low specificity in mRNA expression levels of *GPX7* in the human body, including tissues and cell lines.

mRNA expression levels of *GPX7* in human tumor tissues

Figure 2 shows that mRNA expression levels of *GPX7* were elevated in various human tumor tissues compared to normal tissues. Specific as follows：In Figure 2A：the mRNA expression levels of *GPX7* were elevated in Adrenocortical carcinoma (ACC), Bladder Urothelial Carcinoma (BLCA), Breast invasive carcinoma (BRCA), Cholangiocarcinoma (CHOL), Lymphoid Neoplasm Diffuse Large B-cell Lymphoma(DLBC), Esophageal carcinoma(ESCA). In Figure 2B, the mRNA expression levels of *GPX7* were elevated in Glioblastoma multiforme (GBM), Head and Neck squamous cell carcinoma (HNSC), Kidney renal clear cell carcinoma (KIRC), Kidney renal papillary cell carcinoma (KIRP), LGG, Liver hepatocellular carcinoma (LIHC). As is shown in figure 2C：the mRNA expression levels of *GPX7* were elevated in Lung adenocarcinoma (LUAD), Lung squamous cell carcinoma (LUSC), Ovarian serous cystadenocarcinoma (OV), Pancreatic adenocarcinoma (PAAD), Pheochromocytoma and Paraganglioma (PCPG), Rectum adenocarcinoma (READ). As is shown in figure 2D, the mRNA expression levels of *GPX7* were elevated in Skin Cutaneous Melanoma (SKCM), Stomach adenocarcinoma (STAD), Testicular Germ Cell Tumors (TGCT), Thyroid carcinoma (THCA), Uterine Corpus Endometrial Carcinoma (UCEC), and Uterine Carcinosarcoma (UCS). In the above results all $ps < 0.01$. In contrast, *GPX7* mRNA expression levels were under-expressed in some tumor types, including: Cervical squamous cell carcinoma and endocervical adenocarcinoma (CESC), Colon adenocarcinoma (COAD), and Prostate adenocarcinoma (PRAD).

Association between GPX7 protein expression and pathological parameters

Expression sequences of the GPX7 protein in different tumor types are shown in Figure 3A. Similar to *GPX7* mRNA expression, GPX7 protein expression levels were found to be overexpressed in BRCA, COAD, KIRC, UCEC and LUAD. Figure 3B shows that there were differences in the pathological stages of BLCA and UCS tumors (both $p < 0.05$). In BLCA, GPX7 protein was highly expressed in phase III and lowest in phase II. In UCS, expression of GPX7 protein was highest in phase II and lowest in phase I.

Associations between other pathological parameters and GPX7 protein expression are shown in Figure 4. In Figure 4A, expression levels of the GPX7 protein exhibited a gradually increasing trend in BRCA, OV, COAD, KIRC, UCEC and LUAD. That is, the highest expression was found in stage IV. In both BRCA and LUAD, the gradually increasing with disease progression was not observed, possibly due to insufficient sample size. In Figure 4B, expression levels of the GPX7 protein in OV, COAD, KIRC, UCEC and LUAD were generally elevated in Caucasian races than in other races. In Figure 4C, in terms of age, elevated expression levels of the GPX7 protein were closely correlated with BRCA, OV, COAD, KIRC, and UCEC in people aged 20 to 40 years. In Figure 4D, in terms of gender, expression levels of the GPX7 protein in COAD and LUAD patients were elevated in males than in females, while in UCEC, expression levels of the GPX7 protein were elevated in females than in males.

Survival and prognosis analysis data

Survival map and Kaplan-Meier Survival plots are shown in Figure 5. Figure5A shows that *GPX7* expression was correlated with overall survival (OS) in LGG (p = 4.4e-08), LIHC (p = 0.022), Mesothelioma (MESO) (p = 4e-04), Sarcoma (SARC) (p = 0.015) and STAD (p = 0.0096). Elevated expression levels of *GPX7* were correlated with poor prognosis. Figure 5B shows that expression levels *GPX7* were correlated with disease-free survival (DFS) in LGG (p = 3.6e-05), SARC (p = 0.015) and STAD (p = 0.0096), THCA (p = 0.039). In addition, elevated expression levels of *GPX7* were associated with a prognostic disadvantage. while the level of *GPX7* expression in THCA was not significantly different from that in DFS.

Figure 6 shows that changes in *GPX7* expression levels were associated with OS, DFS progression free survival (PFS)and disease specific survival (DSS). In general, elevated *GPX7* expression levels were associated with a prognostic disadvantage in most tumors. Figure 6A, 6B and 6C, elevated expression levels of *GPX7* were significantly associated with prognostic disadvantages in BLCA, Kidney Chromophobe (KICH), LGG, SARC, and STAD regarding OS, DFS and PFS, implying that the higher the expression, the worse the prognosis. In contrast, elevated expression levels of *GPX7* in Thymoma (THYM) were correlated with better OS and PFS outcomes. These findings imply that overexpression of *GPX7* is correlated with survival disadvantages in cancer patients (THYM exempted). As shown in figure 6D, *GPX7* expression levels were not closely related to DSS in tumors. Based on the above data, we evaluated the relationship between *GPX7* and LGG. OS, DFS and PFS strongly supported that the prognosis of LGG was worse when *GPX7* expression levels were elevated. Therefore, our subsequent analyses focused on LGG.

Association between *GPX7* mRNA expression levels and Tumor Mutation Burden(TMB) / Microsatellite instability(MSI)

Figure 7A shows that the expression level of *GPX7* was negatively correlated with TMB in most cancers. Among them, the statistically significant results are as follows:

PRAD (r = −0.336, p = 4.31e-14), STAD (r = −0.284, p = 3.26e-08), Uveal Melanoma (UVM) (r = −0.249, p = 0.026), ESCA (r = −0.24, p = 0.002), THYM(r = −0.223, p = 0.016), SKCM(r = −0.196, p = 2.26e-05), LIHC(r = −0.171, p = 0.002), PAAD(r = −0.16, p = 0.043), HNSC(r = −0.14, p = 0.001), COAD(r = −0.11, p = 0.039) and THCA(r = −0.109, p = 0.017).However, there was a positive correlation between *GPX7* expression level and OV (r = 0.148, p = 0.019), LGG (r = 0.366, p = 1.15e-17) in terms of TMB.

Figure 7B shows that there was a negative correlation between *GPX7* and MSI in DLBC (r = −0.296, p = 0.041), STAD (r = −0.221, p = 1.58e-05), LUAD (r = −0.191, p = 1.35e-05) and LUSC (r = −0.114, p = 0.011). While, in TGCT (r = 0.18, p = 0.038), the expression level of *GPX7* was positively correlated with MSI. The above results were statistically significant.

Immune infiltration analysis

The immune microenvironment plays key roles in tumor progression and elimination. Therefore, it is important to evaluate the association between *GPX7* expression and the pro-/anti-tumor immune components. Then, we used the EPIC algorism to quantify the density of several important immune cells in each cancer type, which were then correlated with *GPX7* expression levels. Figure 8A shows that there was an overall positive correlation between endothelial cell, macrophage and *GPX7* expression levels in pan-cancers. Expression levels of *GPX7* was positively correlated with macrophage, endothelial cell and B cell infiltrations in BRCA, COAD, HNSC, PAAD and STAD. In PRAD, the expressions of *GPX7* were significantly positively correlated with CD4+T cell, CD8+T cell, macrophage, colorectal cell and B cell infiltrations. In LGG, *GPX7* expression was negatively correlated with CD4+T cell, CD8+T cell and B cell infiltrations. It was positively correlated with macrophage infiltrations.

The relationship between *GPX7* and immune infiltrations of CAFs in tumors is shown in Figure 8B. Based on the four algorithms of TIDE, XCELL, EPIC, and MCPCOUNTER, we found that *GPX7* expression levels and CAFs abundances were positively correlated in most cancer types (BLCA, BRCA, BRCA-LumA, BRCA-LumB, CESC, COAD, ESCA, HNSC, HNSC-HPV-, HNSC-HPV+, LGG, LUAD, LUSC, MESO, PAAD, PRAD, READ, SKCM-Metastasis, STAD, and TGCT). However, based on XCELL algorisms, there was a significant negative correlation between *GPX7* expression and CAFs in DLBC. Further, we focused on the relationship between *GPX7* and endothelial cell, macrophage, and CAFs in tumorigenesis.

Enrichment analysis of *GPX7*-related genes

Enrichment analysis of a series of pathways in which GPX7-binding protein and *GPX7* expression related genes are involved is conducive to further evaluation of the molecular mechanisms of the *GPX7* gene in tumorigenesis. Figure 9A shows the protein-protein interaction (PPI) network between these genes and proteins. Analysis of the top 100 similar genes revealed that the expression of *GPX7* was positively correlated with *MFAP2, P3H1, CHST14, SERPINH1* and *FKBP7* (Figure 9B). Then, we performed Kyoto Encyclopedia of Genes and Genomes (KEGG) pathway analysis of these genes using the STRING

database (Figure 9C). The KEGG pathway analysis revealed that most of the terms were enriched in metabolic pathways, including glutathione metabolism, drug metabolism- cytochrome P450, platinum drug resistance, metabolism of xenobiotics by cytochrome P450, chemical carcinogenesis, and drug metabolism-other enzymes. Figure 9D shows that the genes co-expressed with *GPX7* were mainly involved in the glutathione derivative biosynthetic and glutathione metabolic biological processes. The most overrepresented Gene Ontology (GO) term was the endoplasmic reticulum lumen. Main molecular functions of *GPX7*-associated genes were mainly concentrated in the glutathione transferase activity.

The established nomogram was a better prognostic model for LGG

As shown in Figure 10A and 10B, the independent prognostic factors for LGG patients, including age, gender, and race were screened by univariate and multivariate regression analysis. As independent prognostic parameters, age, gender, and race, were incorporated in the prognostic nomogram to predict 2,3, and 5-year OS (Figure 10C). The concordance index(C-index) of the nomogram was 0.845 (95% CI, 0.825 to 0.865; $p < 0.001$). Calibration plots (Figure 10D) revealed a good agreement between nomogram prediction and actual observation in terms of the 1,2,3 and 5-year OS. Clinical prognostic values of *GPX7* were evaluated using clinical survival data from the TCGA database. *GPX7* was found to be highly expressed and was associated with poor OS in LGG.

Discussion

The occurrence and development of cancer is a major public health problem, and it continues to bring a huge economic and social burden. The etiologic factors for cancer have not been fully established, its pathogenesis is complicated while its prognosis is poor. Therefore, studies should aim at identifying effective tumor markers that can inform the survival prognosis of cancer patients. *GPX7* is involved in the progression of many diseases. However, it has not been extensively evaluated in various tumors. Therefore, it is important to establish the role of *GPX7* in tumor prognosis, progression and treatment.

ROS are involved in tumor occurrence and development. As a normal internal product of the body, ROS is produced through different mechanisms: such as signal transduction factors in the cytoplasm [15], oxidative respiration in the mitochondria and oxidative protein folding in the endoplasmic reticulum [16], external stimuli, such as ultraviolet radiation [17] and viral infection [18]. The balance of the internal ROS levels plays a key role in maintaining cell homeostasis [19]. Normal cells have a complete antioxidant system through which they protect against ROS-associated DNA damage [20–22]. When there is an imbalance between ROS production and the biological detoxification process, the body produces an oxidative stress response. A certain threshold of oxidative stress promotes tumorigenesis by regulating multiple signaling pathways during cell development. However, excessive oxidative stress can cause oxidative damage and even tumor cell death [23, 24]. How tumor cells choose the role of ROS to promote or inhibit apoptosis is still unclear. and it may be associated with the mutation of functional p53 and NF-

kB [25]. The body's oxidative stress responses are associated with the occurrence and development of tumors, and plays a dual role in promoting cancer and as anti-cancer.

As one of the three most important enzyme families in ROS elimination, *GPXs* plays an important role in the antioxidant system by scavenging hydrogen peroxide (H_2O_2), organic peroxides and lipid peroxides [22]. *GPX7*, a newly discovered non-selenium-containing member of the *GPX* family, is free near the endoplasmic reticulum and is one of the proteins with glutathione peroxidase activity [4] [26]. It has a high amino acid sequence homology with other family members [3, 5]. It has been reported that after *GPX7* knockout in mice they developed various abnormalities, such as high cancer incidences, systemic oxidative stress damage, and short lifespan [26]. However, it has also been found that *GPX7* expression is elevated in hepatocellular carcinoma [11]. Therefore, the role of *GPX7* in cancer should be further elucidated. Based on our pan-cancer data analysis, we hypothesized that *GPX7* plays different roles at different stages of different tumors, and it may play a dual role in both carcinogenesis and anticancer. It has been shown that the GPXs family play different roles in tumor occurrence and development [27–31]. Pan-cancer analysis revealed that the expression of *GPX7* was elevated in most tumor tissues when compared to normal tissues. Another study found that *GPX7* expression was elevated in hepatocellular carcinoma LIHC [11]. In this study [11], *GPX7* expression in liver cirrhosis associated with hepatitis C virus (HCV) and Hepatocellular carcinoma (HCC)was evaluated by immunohistochemistry and RT-qPCR analysis in 30 paraffin sections from liver biopsy pathogens. The results showed that *GPX7* was significantly higher in HCC tissues than in liver cirrhosis tissues, and the difference was statistically significant. Moreover, their expression in stage HCC tissues were significantly higher than that in stage I- HCC tissues. Thus, the expression of *GPX7* was proposed as a possible marker for the diagnosis/prognosis of HCC. These findings are consistent with ours, which revealed that *GPX7* function is active in these tumors. In addition, we confirmed that *GPX7* expression was correlated with tumor stage. As the disease progressed, mRNA and protein expression levels of *GPX7* exhibited an upward trend and there was a certain correlation with race, age and gender.

It has been postulated that the function of *GPX7* in cancer cells is to inhibit cancer occurrence, and this does not contradict the above results. Previous studies have shown once *GPX7* was missing or dysfunctional, the body's ROS levels were increased, and esophageal cells are oxidatively damaged by DNA, which will increase the chance of Barrett's oesophagus and oesophageal adenocarcinoma (OAC) [32]. Peng et al. reported that *GPX7* is silenced by DNA hypermethylation during Barrett's oesophageal carcinogenesis. They used quantitative real-time PCR (qRT-PCR) to show that the expressions of pro-inflammatory cytokines (TNF-α, IL-1β, IL-6, and IL-8) and chemokines (CXCL-1 and CXCL-2) were significantly increased in esophageal cells exposed to acidic (pH4) or neutral (pH7) bile salts. The expression of cytokines (TNF-α, IL-1β and IL-8) in esophageal adenocarcinoma tissues was significantly overexpressed compared with that in normal tissues by qRT-PCR, and the expression of cytokines was negatively correlated with the expression of *GPX7*. In other words, the loss of *GPX7* expression could be considered to promote the activity of bile salt-induced pro-inflammatory cytokines and chemokines, leading to the occurrence of Barrett's esophageal cancer [33]. It was found that *GPX7*-deficient mice

developed sporadic cancers, including lung adenocarcinoma (16.7%), leukemia (6.3%), breast carcinoma (5%), sarcoma (6.3%), and lymphoma (T-, B-, or mixed-cell. 61.1%) [34]. The results of our pan-cancer analysis speculated that *GPX7* could inhibit the occurrence of tumors, possibly through the protective effect on oxidative stress. For example, in Barrett's oesophagus and oesophageal adenocarcinoma (OAC), *GPX7* expressed esophageal adenocarcinoma cells could significantly increase the viability and reduce apoptosis during H_2O_2 treatment. On the other hand, *GPX7* deficiency plays a role in tumorigenesis, which may be achieved by inhibiting NF-kB activation in a non-ROS-dependent manner [26]. However, due to some limitation such as small sample size, we could not make a tangible conclusion.

Elevated expression levels of *GPX7* were also associated with a prognostic disadvantage in certain tumors, such as LGG, SARC, and STAD. It has also been reported the expression levels of *GPX7* in glioma tissues were higher than those in normal brain tissues. Elevated expression levels of *GPX7* led to poor prognosis of glioma patients [10]. These findings are consistent with ours. In GBM and LGG tissues, we found that expression levels of *GPX7* were significantly elevated than those in normal tissues. The expression of *GPX7* was negatively correlated with OS, DFS and PFS in LGG ($p < 0.0001$). Finally, we used relevant prognostic factors to establish a nomogram to verify the correctness of the above results. Calibration plots revealed a good agreement between the nomogram prediction and actual observations in terms of the 1,2,3 and 5-year survival rates. A nomogram is a powerful tool that has been widely used to predict an individual's prognosis [35, 36]. We believe that *GPX7* may be used as a therapeutic target for LGG in the future. At the same time, given the elevated expression levels of *GPX7* in most tumor tissues, and through univariate and multivariate linear regression analysis, we postulated that *GPX7* has a pro-cancer role in some tumors. It is expected to be one of the biochemical indices for clinical diagnosis. There is a need to confirm these postulates through clinical experiments.

TMB refers to the number of mutations that exist within a tumor. It is an emerging biomarker of sensitivity to immune checkpoint inhibitors and it can be used to predict some certain tumors, such as lung cancer, malignant melanoma and bladder cancer, and it can help patients benefit from immunotherapy [37, 38]. Microsatellites are widely distributed DNA repetitive motifs. MSI was due to defects in the mismatch repair system, which leads to the accumulation of DNA replication errors and leads to the instability of microsatellites. Studies have shown that MSI is closely associated with the occurrence, progression and prognosis of many malignant tumors [39]. Through pan-cancer analysis, we found that *GPX7* was negatively correlated with TMB/MSI in most tumors. We speculate that when tumors occur in the body, the level of ROS in tumor cells is increased to maintain tumor proliferation, and the increased expression of *GPX7* in cells can alleviate the damage of ROS to the body cells, thereby TMB/MSI were inhibited. At the same time, we postulate that the correlation between *GPX7* and TMB/MSI may be associated with the clinical stage of the tumor. However, research on this is relatively lacking. Further studies should be performed to determine the explicit regulatory mechanisms.

Tumor pathogenesis is an extremely complex physiological and biochemical process. The tumor microenvironment (TME) is widely associated with tumor progression. The TME is a carrier of tumor cells and it interacts with the surrounding cells through the circulatory and lymphatic systems, thereby

affecting cancer development and progression [40]. The TME is made up of different cellular components, including endothelial cells, immune cells, macrophages, and fibroblasts among others. Endothelial cells play an important role in the development of tumors. Development of the tumor-associated neovasculature usually occurs from endothelial progenitor cells and new vessels from existing blood vessels. Through this process, these cells provide nutrients and oxygen to the tumor tissue, thereby promoting its development. The TME is also composed of immune cells, for instance neutrophils, lymphocytes, and macrophages. These cells are closely associated with inflammatory responses during tumor development [41]. In addition, macrophages can assist escaped tumor cells to enter the circulatory system and further inhibit the anti-tumor immune response [42]. In some tumors, especially in digestive tract tumors, such as COAD, PAAD, READ, and STAD, we found that *GPX7* was positively correlated with macrophage, endothelial cell and B cell infiltrations. Therefore, we speculate that there is a close relationship between the occurrence and development of digestive tumors and ROS, which has been supported by relevant studies (colorectal cancer [43], pancreatic cancer [44], gastric cancer [45], etc.). Macrophages and endothelial cells, as important components of the tumor microenvironment, are positively correlated with *GPX7* in some tumors. Whether this phenomenon inhibits or promotes tumor occurrence and development of tumors has not been determined yet. Elevated levels of immune cells could be attributed to: i. *GPX7*, as one of the most important enzymes in ROS elimination process, a certain threshold of *GPX7* in tumor tissues has a strong anti-inflammatory antioxidant role, which may be in the form of increased compensatory participate in tumor immune process. At this point, *GPX7* protects cells from ROS production, oxidative stress, and oxidative DNA damage. When this threshold is exceeded, it may be involved in tumor development with other tumor cells. ii. The role of *GPX7* in human tumors is depend on tumor types and stages, such as digestive tract tumors with severe oxidative damage, and *GPX7* may be hijacked by their associated immune cells, thereby promoting tumor occurrence and development. In addition, it has been reported that the immune system has a dual role, it antagonizes and promotes tumor development and progression [41], which also supports our hypothesis.

Fibroblasts are also important TME components. They provide a pathway for endothelial cells to form blood vessels because it allows cancer cells to move around the body through the bloodstream [46, 47]. Fibroblast responses to tissue damage caused by cancer cells is an important component of the host responses. CAFs interact with tumor cells to promote their proliferation, survival and maintain their malignant state. Tumor cells affect the recruitment of CAF precursors and induce the activation of normal fibroblasts into CAFs [48]. Pan-cancer analysis revealed that *GPX7* was positively correlated with the majority of human tumor CAFs. We hypothesize that *GPX7* plays a pro-cancer role. The reason may be that after exceeding the threshold, *GPX7* has a synergistic effect with other tumor cells, and it is recruited by CAFs to form tumor-related stroma, thus becoming an active participant in tumorigenesis rather than a passive bystander. Fibroblasts are the toughest cells in the body, and they can survive severe stress that is usually fatal to other cells [49]. Therefore, we postulate that *GPX7* has a synergistic effect with CAFs in most tumors, and may be hijacked by powerful CAFs to participate in tumor development and progression.

Given that *GPX7* is significantly overexpressed in most tumors and is closely associated with tumor grade and patient prognosis, we investigated its potential role in cancers. Through GO and KEGG analysis, we found that metabolic processes were the most enriched. These pathways included, glutathione metabolism, drug metabolism- cytochrome P450, platinum drug resistance, metabolism of xenobiotics by cytochrome P450, chemical carcinogenesis, Drug metabolism – other enzymes. Surprisingly, *GPX7* was co-expressed with members of the cytochrome P450 (CYP) family, which is primarily responsible for cancer drug metabolism [50]. Glutathione (GSH) is an abundant antioxidant that exists in organisms whose main function is to maintain cellular redox homeostasis. Glutathione metabolism plays a dual role (beneficial or pathogenic) in a variety of malignancies [51], and it has been extensively studied as a target for cancer treatment [52–54]. Interference with different steps in glutathione metabolism could be used for therapeutic purposes. *GPX7* holds promise for the use of glutathione metabolism for tumor guided therapy in cancer patients.

This study has some limitations: First, all parameters and information were obtained from databases such as TCGA, which are limited and incomplete. Second, analytical data on *GPX7* expression are based on mRNA levels, and conclusions of this study are derived from bioinformatics analysis, which lacks experimental data support. Therefore, more studies are needed to verify our results and to investigate the biological functions of *GPX7*, which will make our conclusions to be reliable and generalizable.

In conclusion, we elucidate on the expression of *GPX7* across human cancers. *GPX7* is upregulated in multiple tumors. Elevated expression levels of *GPX7* are a marker for poor prognosis in LGG patients, therefore, *GPX7* is a potential prognostic indicator for LGG. Additionally, *GPX7* expression was found to be positively correlated with CAFs. In COAD, PAAD, PRAD, READ, and STAD, *GPX7* expression was positively correlated with macrophage and endothelial cell infiltration. Finally, there is a strong correlation between *GPX7* expression and glutathione metabolic pathways. *GPX7* holds promise for the use of glutathione metabolism for guided therapy in cancer patients. Therefore, this study provides a basis for further evaluation of the role of *GPX7* in clinical tumors. In conclusion, *GPX7* regulates tumorigenesis and has a clinical value for the prognosis and treatment of cancer patients.

Materials And Methods

GPX7 expression profiles in human normal tissues and cell lines

The Human Protein Atlas (HPA; https://www.proteinatlas.org/) [55] database was used to evaluate *GPX7* mRNA expression and distribution in human normal tissues and all cell lines. The HPA core is its unique antibody collection, which through immunohistochemistry and immunocytochemistry, can be used to map the entire human proteome. HPA has been used to study protein localization and expression in human tissues and cells. Normalized expression (NX), calculated for each gene in every sample, is used to estimate mRNA expression levels.

GPX7 expression patterns in human tumor tissues

To determine *GPX7* expression differences between tumor tissues and corresponding normal tissues across different cancer types, we downloaded the RNA-seq data for 33 cancer types with matched normal samples from The Cancer Genome Atlas (TCGA; http://cancergenome.nih.gov) [14]. Then, mRNA expression data for normal tissues were downloaded from the Genotype-Tissue Expression project (GTEx; https://gtexportal.org/home) [56], and combined with TCGA data to enlarge sample sizes for normal controls. Raw expression data were log2 transformed [TPM (Transcripts per million) +1] and compared between cancer and normal tissues by *t*-test. Data were visualized as violin plots, and $p < 0.05$ was considered statistically significant.

Association between GPX7 protein expression levels and clinicopathological parameters

From the UALCAN database [57] (http://ualcan.path.uab.edu/analysis-prot.html), we obtained available data sets for six tumors: BRCA, OV, COAD, KIRC, UCEC and LUAD. Analysis data of GPX7-relevant proteomic characteristics, such as tumor stage, age, race and gender were downloaded from the "CPTAC Analysis" module of UALCAN. Z-values represent standard deviations (SD) from the median (M) across

samples of a given cancer and they were used to assess GPX7 protein expressions between cancer and healthy tissues.

Survival and prognosis analysis

The "Survival map" module of the Gene Expression Profiling Interactive Analysis (GEPIA2)[58] (http://gepia.cancer-pku.cn/index.html) was used to obtain OS and DFS significant survival curves of *GPX7* in TCGA tumors. The cutoff-high (50%) and cutoff-low (50%) values were defined as thresholds to group the whole cohort into high and low expression groups respectively. Kaplan-Meier survival plots were established by the "survival analysis" module of GEPIA2. Log-rank test was used to perform hypothesis testing, and determine differences between log-rank test curves.

The *GPX7* mRNA sequencing data from TCGA and GETx databases, univariate Cox regression analysis and forest plots were used to calculate and display hazard ratios (HR) of *GPX7* with 95% confidence interval (95%CI) for each tumor, including OS, DFS, PFS and DSS. $p < 0.05$ was considered statistically significant.

Gene mutation analysis

The tumor RNA-seq data of 33 cancer patients and matched normal tissue samples were downloaded from the Genomic Data Commons (GDC) (https://portal.gdc.cancer.gov/) [59] data portal website of the TCGA database. TMB refers to the number of mutations present in a tumor. It is an emerging immune checkpoint inhibitor sensitive biomarker [60]. Microsatellites are widely distributed DNA repetitive motifs. MSI occurs due to defects in the mismatch repair system, leading to the accumulation of DNA replication errors and microsatellites instability [39]. TMB and MSI are effective prognostic biomarkers and immunotherapeutic response indicators for a variety of tumors. Data for TCGA tumors with *GPX7* gene mutations were used to evaluate the correlation between *GPX7* and TMB/MSI. Statistical analysis was performed using the R software V4.0.3, and the data of the two groups were tested by rank sum test. $p < 0.05$ was considered statistically significant.

Correlation between *GPX7* and infiltration of immune cells

Pan-cancer data from the GDC portal of the TCGA database were analyzed by Immunedeconv[61], a software package that integrates six of the latest algorithms, namely CIBERSORT, CIBERSORT-abs, EPIC, MCP-counter, quanTIseq, TIMER and xCELL. In this study, Estimating the Proportions of Immune and Cancer cells (EPIC) algorithm was used to evaluate the potential relationship between immune cell infiltration levels and expression levels of *GPX7* in TCGA tumors. The EPIC algorithm was based on a reference profile of gene expression of RNA sequences from immune cells and other non-malignant cell types in tumors. EPIC overcomes several limitations of previous methods of predicting cancer and immune cells or other non-malignant cell types from a large amount of tumor gene expression data, taking into account non-characteristic and potentially highly variable cell types [62]. R software V4.0.3 was used for statistical analysis, and $p < 0.05$ was considered statistically significant.

The Tumor Immune Estimation Resource (TIMER) [63] (http://timer.cistrome.org/) is an interactive web application that is used to comprehensively and flexibly analyze the richness of tumor infiltrating immune cells (TIICs). The “Gene” module of TIMER 2.0 was used to determine the association between gene expression and immune cell infiltration in the TCGA datasets. For our purposes, only Cancer-associated fibroblasts (CAFs) were screened for analysis. Immune infiltration levels were estimated by algorithms including EPIC, MCPCOUNTER, XCELL and TIDE. When the results of four algorithms were all statistically significant, a scatter plot with the highest correlation coefficient was given. CAFs are important components in the tumor microenvironment, which play an essential role in tumor progression. It has been shown that CAFs do not exist as individual cells around the tumor. Instead, they interacts with tumor cells to promote tumor progression, survival and maintain its malignant properties [64]. R software V4.0.3 was used for statistical analysis. The rank-sum test was used to compare data of the two groups, $p < 0.05$ was considered statistically significant.

Enrichment analysis of *GPX7*-related genes

The “Similar Gene Detection” module of GEPIA2 was used to obtain the top 100 *GPX7*-correlated target genes. The "Correlation Analysis" module of GEPIA2 was used for Pearson Correlation Analysis of *GPX7* gene pairs, and the top 5 genes were screened out. The data used in the analyses were obtained from all TCGA tumor and normal tissue datasets. The log2 TPM was applied for the dot plot. *p*-value and the correlation coefficient (R) were indicated.

For our purposes, the first 50 GPX7-binding proteins were obtained from the "Multiple protein" module of the STRING website [65] (https://string-db.org/). Important parameters were: List of Names (“*GPX7*”) and organism (“Homo sapiens”), minimum required interaction score [“Low confidence (0.150)”], and max number of interactors to show (“no more than 50 interactors” in 1st shell).

Subsequently, two sets of gene data were input in the “Multiple protein” module of the STRING website. Important parameters were: Minimum required interaction score [" High confidence (0.70) "]. The PPI network of *GPX7*-related gene was established, and analysis lists of KEGG, Biological processes (BP), Molecular function (MF), Cellular component (CC) were obtained in the “Analysis module”. GO and KEGG terms with false discovery rate (FDR)-corrected Q-values less than 0.05 were considered significantly enriched. For displaying purposes, the top 10 GO terms of each three GO domains-BP, CC, MF, and the top 20 KEGG pathway terms were presented as in a bubble chart.

Prognostic nomogram for LGG

To further validate the correlation between *GPX7* mRNA expression levels and cancer occurrence, independent prognostic factors for LGG patients were determined by performing univariate and multivariate cox regression analysis with Cox proportional hazards regression. The p value, HR, and 95% CI of each variable were displayed using forest plots. Then, based on findings of multivariate Cox regression proportional hazards analysis, we constructed a nomogram to predict the 2, 3, and 5years OS of LGG patients. A concordance index (C-index) was used to evaluate the judgment of nomogram. The nomogram calibration curve was constructed and validated by comparing predicted OS to observed OS.

Abbreviations

GPX7: Glutathione peroxidase-7

TCGA: The Cancer Genome Atlas

GTEx: Genotype-Tissue Expression

GDC: Genomic Data Commons

GEPIA: Gene Expression Profiling Interactive Analysis

TIMER: Tumor Immune Estimation Resource

HPA: Human Protein Atlas

ROS: Reactive Oxygen Species

OS: overall survival

DFS: disease-free survival

PFS: progression-free survival

DSS: disease specific survival

HCC: Hepatocellular carcinoma

HR: Hazard ratio

95%CI: 95% confidence intervals

TIICs: tumor infiltrating immune cells

PPI: protein-protein interaction

ACC: Adrenocortical carcinoma

BLCA: Bladder Urothelial Carcinoma

BRCA: Breast invasive carcinoma

CESC: Cervical squamous cell carcinoma and endocervical adenocarcinoma

CHOL: Cholangiocarcinoma

COAD: Colon adenocarcinoma

DLBC: Lymphoid Neoplasm Diffuse Large B-cell Lymphoma

ESCA: Esophageal carcinoma

GBM: Glioblastoma multiforme

HNSC: Head and Neck squamous cell carcinoma

KICH: Kidney Chromophobe

KIRC: Kidney renal clear cell carcinoma

KIRP: Kidney renal papillary cell carcinoma

LGG: Brain Lower Grade Glioma

LIHC: Liver hepatocellular carcinoma

LUAD: Lung adenocarcinoma

LUSC: Lung squamous cell carcinoma

MESO: Mesothelioma

OV: Ovarian serous cystadenocarcinoma

PAAD: Pancreatic adenocarcinoma

PCPG: Pheochromocytoma and Paraganglioma

PRAD: Prostate adenocarcinoma

READ: Rectum adenocarcinoma

SARC: Sarcoma

SKCM: Skin Cutaneous Melanoma

STAD: Stomach adenocarcinoma

TGCT: Testicular Germ Cell Tumors

THCA: Thyroid carcinoma

THYM: Thymoma

UCEC: Uterine Corpus Endometrial Carcinoma

UCS: Uterine Carcinosarcoma

UVM: Uveal Melanoma

TMB: Tumor Mutation Burden

MSI: Microsatellite Instability

TME: Tumor Microenvironment

EPIC: Estimating the Proportions of Immune and Cancer cells

GO: Gene Ontology

KEGG: Kyoto Encyclopedia of Genes and Genomes

BP: biological process

MF: molecular function

CC: cell component

Declarations

Acknowledgements

Not applicable

Authors' contributions

QZ, YY and RZ conceived and designed the study; LZ, YW, TW, YS and JC collected and assembled data; MQ, XD and ZX performed data analysis; QZ and YY drafted the manuscript; QZ, YY and RZ participated in study supervision and commented on the manuscript. RZ funded acquisition. All authors reviewed the manuscript.

Funding

This study was supported by Special R&D Program Project of Chinese Academy of Se-enriched Industry (2020FXZX05-01), Key Research and Development Program of Shaanxi Province (2020SF-076), Research Project from Health Commission of Shaanxi Provincial Government (2018A017), Education Department of Shaanxi Provincial Government (19JS015).

Availability of data and materials

The datasets analyzed during the current study are available in the TCGA database (http://cancergenome.nih.gov) and the GTEx database(https://gtexportal.org/home)

Ethics approval and consent to participate

Not applicable.

Consent for publication

Not applicable.

Competing interests

The authors declare no conflict of interests.

References

1. World Health Organization (WHO). Global Health Estimates(GHE). 2020. https://www.who.int/healthinfo/global-burden-disease/en/. Accessed 21 May 2021.
2. World Health Organization (WHO). World cancer report 2020. https://www.iarc.fr/cards_page/world-cancer-report/. Accessed 21 May 2021.
3. Utomo A, Jiang X, Furuta S, Yun J, Levin DS, Wang YC, et al. Identification of a novel putative non-selenocysteine containing phospholipid hydroperoxide glutathione peroxidase (NPGPx) essential for alleviating oxidative stress generated from polyunsaturated fatty acids in breast cancer cells. J Biol Chem. 2004;279(42):43522–9.doi:10.1074/jbc.M407141200.
4. Nguyen VD, Saaranen MJ, Karala AR, Lappi AK, Wang L, Raykhel IB, et al. Two endoplasmic reticulum PDI peroxidases increase the efficiency of the use of peroxide during disulfide bond formation. J Mol Biol. 2011;406(3):503–15.doi:10.1016/j.jmb.2010.12.039.
5. Toppo S, Vanin S, Bosello V, Tosatto SC. Evolutionary and structural insights into the multifaceted glutathione peroxidase (Gpx) superfamily. Antioxid Redox Signal. 2008;10(9):1501–14.doi:10.1089/ars.2008.2057.
6. Brigelius-Flohe R, Maiorino M. Glutathione peroxidases. Biochim Biophys Acta. 2013;1830(5):3289–303.doi:10.1016/j.bbagen.2012.11.020.
7. Bosello-Travain V, Conrad M, Cozza G, Negro A, Quartesan S, Rossetto M, et al. Protein disulfide isomerase and glutathione are alternative substrates in the one Cys catalytic cycle of glutathione peroxidase 7. Biochim Biophys Acta. 2013;1830(6):3846–57.doi:10.1016/j.bbagen.2013.02.017.
8. Chen Z, Hu T, Zhu S, Mukaisho K, El-Rifai W, Peng DF. Glutathione peroxidase 7 suppresses cancer cell growth and is hypermethylated in gastric cancer. Oncotarget. 2017;8(33):54345–56.doi:10.18632/oncotarget.17527.
9. Peppelenbosch MP, Spaander MC, Bruno MJ. Glutathione peroxidase 7 prevents cancer in the oesophagus. Gut. 2014;63(4):537–8.doi:10.1136/gutjnl-2013-304906.
10. Yao J, Chen X, Liu Z, Zhang R, Zhang C, Yang Q, et al. The increasing expression of GPX7 related to the malignant clinical features leading to poor prognosis of glioma patients. Chin Neurosurg J. 2021;7(1):21.doi:10.1186/s41016-021-00235-3.
11. Guerriero E, Capone F, Accardo M, Sorice A, Costantini M, Colonna G, Castello G, Costantini S. GPX4 and GPX7 over-expression in human hepatocellular carcinoma tissues. Eur J Histochem. 2015;59(4):2540.doi:10.4081/ejh.2015.2540.
12. Clough E, Barrett T. The Gene Expression Omnibus Database. Methods Mol Biol. 2016;1418:93–110.doi:10.1007/978-1-4939-3578-9_5.

13. Blum A, Wang P, Zenklusen JC. SnapShot: TCGA-Analyzed Tumors. Cell. 2018;173(2):530.doi:10.1016/j.cell.2018.03.059.
14. Tomczak K, Czerwinska P, Wiznerowicz M. The Cancer Genome Atlas (TCGA): an immeasurable source of knowledge. Contemp Oncol (Pozn). 2015;19(1A):A68-77.doi:10.5114/wo.2014.47136.
15. Schieber M, Chandel NS. ROS function in redox signaling and oxidative stress. Curr Biol. 2014;24(10):R453-62.doi:10.1016/j.cub.2014.03.034.
16. Malhotra JD, Kaufman RJ. Endoplasmic reticulum stress and oxidative stress: a vicious cycle or a double-edged sword? Antioxid Redox Signal. 2007;9(12):2277–93.doi:10.1089/ars.2007.1782.
17. Bickers DR, Athar M. Oxidative stress in the pathogenesis of skin disease. J Invest Dermatol. 2006;126(12):2565–75.doi:10.1038/sj.jid.5700340.
18. Paracha UZ, Fatima K, Alqahtani M, Chaudhary A, Abuzenadah A, Damanhouri G, Qadri I. Oxidative stress and hepatitis C virus. Virol J. 2013;10:251.doi:10.1186/1743-422X-10-251.
19. D'Autreaux B, Toledano MB. ROS as signalling molecules: mechanisms that generate specificity in ROS homeostasis. Nat Rev Mol Cell Biol. 2007;8(10):813–24.doi:10.1038/nrm2256.
20. Halliwell B. Antioxidant defence mechanisms: from the beginning to the end (of the beginning). Free Radic Res. 1999;31(4):261–72.doi:10.1080/10715769900300841.
21. Strange RC, Spiteri MA, Ramachandran S, Fryer AA. Glutathione-S-transferase family of enzymes. Mutat Res. 2001;482(1–2):21–6.doi:10.1016/s0027-5107(01)00206-8.
22. Brigelius-Flohe R, Kipp A. Glutathione peroxidases in different stages of carcinogenesis. Biochim Biophys Acta. 2009;1790(11):1555–68.doi:10.1016/j.bbagen.2009.03.006.
23. Sosa V, Moline T, Somoza R, Paciucci R, Kondoh H, ME LL. Oxidative stress and cancer: an overview. Ageing Res Rev. 2013;12(1):376–90.doi:10.1016/j.arr.2012.10.004.
24. Sies H, Jones DP. Reactive oxygen species (ROS) as pleiotropic physiological signalling agents. Nat Rev Mol Cell Biol. 2020;21(7):363–83.doi:10.1038/s41580-020-0230-3.
25. Sasaki Y. Does oxidative stress participate in the development of hepatocellular carcinoma? J Gastroenterol. 2006;41(12):1135–48.doi:10.1007/s00535-006-1982-z.
26. Wei PC, Hsieh YH, Su MI, Jiang X, Hsu PH, Lo WT, et al. Loss of the oxidative stress sensor NPGPx compromises GRP78 chaperone activity and induces systemic disease. Mol Cell. 2012;48(5):747–59.doi:10.1016/j.molcel.2012.10.007.
27. Valea A, Georgescu CE. Selenoproteins in human body: focus on thyroid pathophysiology. Hormones (Athens). 2018;17(2):183–96.doi:10.1007/s42000-018-0033-5.
28. Murawaki Y, Tsuchiya H, Kanbe T, Harada K, Yashima K, Nozaka K, et al. Aberrant expression of selenoproteins in the progression of colorectal cancer. Cancer Lett. 2008;259(2):218–30.doi:10.1016/j.canlet.2007.10.019.
29. Burk RF, Olson GE, Winfrey VP, Hill KE, Yin D. Glutathione peroxidase-3 produced by the kidney binds to a population of basement membranes in the gastrointestinal tract and in other tissues. Am J Physiol Gastrointest Liver Physiol. 2011;301(1):G32-8.doi:10.1152/ajpgi.00064.2011.

30. Barrett CW, Ning W, Chen X, Smith JJ, Washington MK, Hill KE, et al. Tumor suppressor function of the plasma glutathione peroxidase gpx3 in colitis-associated carcinoma. Cancer Res. 2013;73(3):1245–55.doi:10.1158/0008-5472.CAN-12-3150.
31. Cejas P, Garcia-Cabezas MA, Casado E, Belda-Iniesta C, De Castro J, Fresno JA, et al. Phospholipid hydroperoxide glutathione peroxidase (PHGPx) expression is downregulated in poorly differentiated breast invasive ductal carcinoma. Free Radic Res. 2007;41(6):681–7.doi:10.1080/10715760701286167.
32. Peng D, Belkhiri A, Hu T, Chaturvedi R, Asim M, Wilson KT, Zaika A, El-Rifai W. Glutathione peroxidase 7 protects against oxidative DNA damage in oesophageal cells. Gut. 2012;61(9):1250–60.doi:10.1136/gutjnl-2011-301078.
33. Peng DF, Hu TL, Soutto M, Belkhiri A, El-Rifai W. Glutathione Peroxidase 7 Suppresses Bile Salt-Induced Expression of Pro-Inflammatory Cytokines in Barrett's Carcinogenesis. J Cancer. 2014;5(7):510–7.doi:10.7150/jca.9215.
34. Chen YI, Wei PC, Hsu JL, Su FY, Lee WH. NPGPx (GPx7): a novel oxidative stress sensor/transmitter with multiple roles in redox homeostasis. Am J Transl Res. 2016;8(4):1626-40.doi.
35. Liang W, Zhang L, Jiang G, Wang Q, Liu L, Liu D, et al. Development and validation of a nomogram for predicting survival in patients with resected non-small-cell lung cancer. J Clin Oncol. 2015;33(8):861–9.doi:10.1200/JCO.2014.56.6661.
36. Han DS, Suh YS, Kong SH, Lee HJ, Choi Y, Aikou S, et al. Nomogram predicting long-term survival after d2 gastrectomy for gastric cancer. J Clin Oncol. 2012;30(31):3834–40.doi:10.1200/JCO.2012.41.8343.
37. Chang L, Chang M, Chang HM, Chang F. Microsatellite Instability: A Predictive Biomarker for Cancer Immunotherapy. Appl Immunohistochem Mol Morphol. 2018;26(2):e15-e21.doi:10.1097/PAI.0000000000000575.
38. Ritterhouse LL. Tumor mutational burden. Cancer Cytopathol. 2019;127(12):735–6.doi:10.1002/cncy.22174.
39. Yang G, Zheng RY, Jin ZS. Correlations between microsatellite instability and the biological behaviour of tumours. J Cancer Res Clin Oncol. 2019;145(12):2891–9.doi:10.1007/s00432-019-03053-4.
40. Arneth B. Tumor Microenvironment. Medicina (Kaunas). 2019;56(1).doi:10.3390/medicina56010015.
41. Hanahan D, Weinberg RA. Hallmarks of cancer: the next generation. Cell. 2011;144(5):646–74.doi:10.1016/j.cell.2011.02.013.
42. Mantovani A, Allavena P, Sica A, Balkwill F. Cancer-related inflammation. Nature. 2008;454(7203):436–44.doi:10.1038/nature07205.
43. Lin S, Li Y, Zamyatnin AA, Jr., Werner J, Bazhin AV. Reactive oxygen species and colorectal cancer. J Cell Physiol. 2018;233(7):5119–32.doi:10.1002/jcp.26356.
44. Durand N, Storz P. Targeting reactive oxygen species in development and progression of pancreatic cancer. Expert Rev Anticancer Ther. 2017;17(1):19–31.doi:10.1080/14737140.2017.1261017.

45. Huang T, Zhou F, Yuan X, Yang T, Liang X, Wang Y, et al. Reactive Oxygen Species Are Involved in the Development of Gastric Cancer and Gastric Cancer-Related Depression through ABL1-Mediated Inflammation Signaling Pathway. Oxid Med Cell Longev. 2019;2019:5813985.doi:10.1155/2019/5813985.
46. Korneev KV, Atretkhany KN, Drutskaya MS, Grivennikov SI, Kuprash DV, Nedospasov SA. TLR-signaling and proinflammatory cytokines as drivers of tumorigenesis. Cytokine. 2017;89:127–35.doi:10.1016/j.cyto.2016.01.021.
47. Das R, Bassiri H, Guan P, Wiener S, Banerjee PP, Zhong MC, Veillette A, Orange JS, Nichols KE. The adaptor molecule SAP plays essential roles during invariant NKT cell cytotoxicity and lytic synapse formation. Blood. 2013;121(17):3386–95.doi:10.1182/blood-2012-11-468868.
48. Kalluri R. The biology and function of fibroblasts in cancer. Nat Rev Cancer. 2016;16(9):582–98.doi:10.1038/nrc.2016.73.
49. Bliss LA, Sams MR, Deep-Soboslay A, Ren-Patterson R, Jaffe AE, Chenoweth JG, Jaishankar A, Kleinman JE, Hyde TM. Use of postmortem human dura mater and scalp for deriving human fibroblast cultures. PLoS One. 2012;7(9):e45282.doi:10.1371/journal.pone.0045282.
50. Zanger UM, Schwab M. Cytochrome P450 enzymes in drug metabolism: regulation of gene expression, enzyme activities, and impact of genetic variation. Pharmacol Ther. 2013;138(1):103 – 41.doi:10.1016/j.pharmthera.2012.12.007.
51. Bansal A, Simon MC. Glutathione metabolism in cancer progression and treatment resistance. J Cell Biol. 2018;217(7):2291–8.doi:10.1083/jcb.201804161.
52. Desideri E, Ciccarone F, Ciriolo MR. Targeting Glutathione Metabolism: Partner in Crime in Anticancer Therapy. Nutrients. 2019;11(8).doi:10.3390/nu11081926.
53. Lv H, Zhen C, Liu J, Yang P, Hu L, Shang P. Unraveling the Potential Role of Glutathione in Multiple Forms of Cell Death in Cancer Therapy. Oxid Med Cell Longev. 2019;2019:3150145.doi:10.1155/2019/3150145.
54. Xiao Y, Meierhofer D. Glutathione Metabolism in Renal Cell Carcinoma Progression and Implications for Therapies. Int J Mol Sci. 2019;20(15).doi:10.3390/ijms20153672.
55. Thul PJ, Lindskog C. The human protein atlas: A spatial map of the human proteome. Protein Sci. 2018;27(1):233–44.doi:10.1002/pro.3307.
56. Carithers LJ, Moore HM. The Genotype-Tissue Expression (GTEx) Project. Biopreserv Biobank. 2015;13(5):307–8.doi:10.1089/bio.2015.29031.hmm.
57. Chandrashekar DS, Bashel B, Balasubramanya SAH, Creighton CJ, Ponce-Rodriguez I, Chakravarthi B, Varambally S. UALCAN: A Portal for Facilitating Tumor Subgroup Gene Expression and Survival Analyses. Neoplasia. 2017;19(8):649 – 58.doi:10.1016/j.neo.2017.05.002.
58. Tang Z, Kang B, Li C, Chen T, Zhang Z. GEPIA2: an enhanced web server for large-scale expression profiling and interactive analysis. Nucleic Acids Res. 2019;47(W1):W556-W60.doi:10.1093/nar/gkz430.

59. Jensen MA, Ferretti V, Grossman RL, Staudt LM. The NCI Genomic Data Commons as an engine for precision medicine. Blood. 2017;130(4):453–9.doi:10.1182/blood-2017-03-735654.
60. Chalmers ZR, Connelly CF, Fabrizio D, Gay L, Ali SM, Ennis R, et al. Analysis of 100,000 human cancer genomes reveals the landscape of tumor mutational burden. Genome Med. 2017;9(1):34.doi:10.1186/s13073-017-0424-2.
61. Sturm G, Finotello F, List M. Immunedeconv: An R Package for Unified Access to Computational Methods for Estimating Immune Cell Fractions from Bulk RNA-Sequencing Data. Methods Mol Biol. 2020;2120:223–32.doi:10.1007/978-1-0716-0327-7_16.
62. Racle J, Gfeller D. EPIC: A Tool to Estimate the Proportions of Different Cell Types from Bulk Gene Expression Data. Methods Mol Biol. 2020;2120:233–48.doi:10.1007/978-1-0716-0327-7_17.
63. Li T, Fan J, Wang B, Traugh N, Chen Q, Liu JS, Li B, Liu XS. TIMER: A Web Server for Comprehensive Analysis of Tumor-Infiltrating Immune Cells. Cancer Res. 2017;77(21):e108-e10.doi:10.1158/0008-5472.CAN-17-0307.
64. Sahai E, Astsaturov I, Cukierman E, DeNardo DG, Egeblad M, Evans RM, et al. A framework for advancing our understanding of cancer-associated fibroblasts. Nature Reviews Cancer. 2020;20(3):174–86.doi:10.1038/s41568-019-0238-1.
65. Szklarczyk D, Gable AL, Lyon D, Junge A, Wyder S, Huerta-Cepas J, et al. STRING v11: protein-protein association networks with increased coverage, supporting functional discovery in genome-wide experimental datasets. Nucleic Acids Res. 2019;47(D1):D607-D13.doi:10.1093/nar/gky1131.

Figures

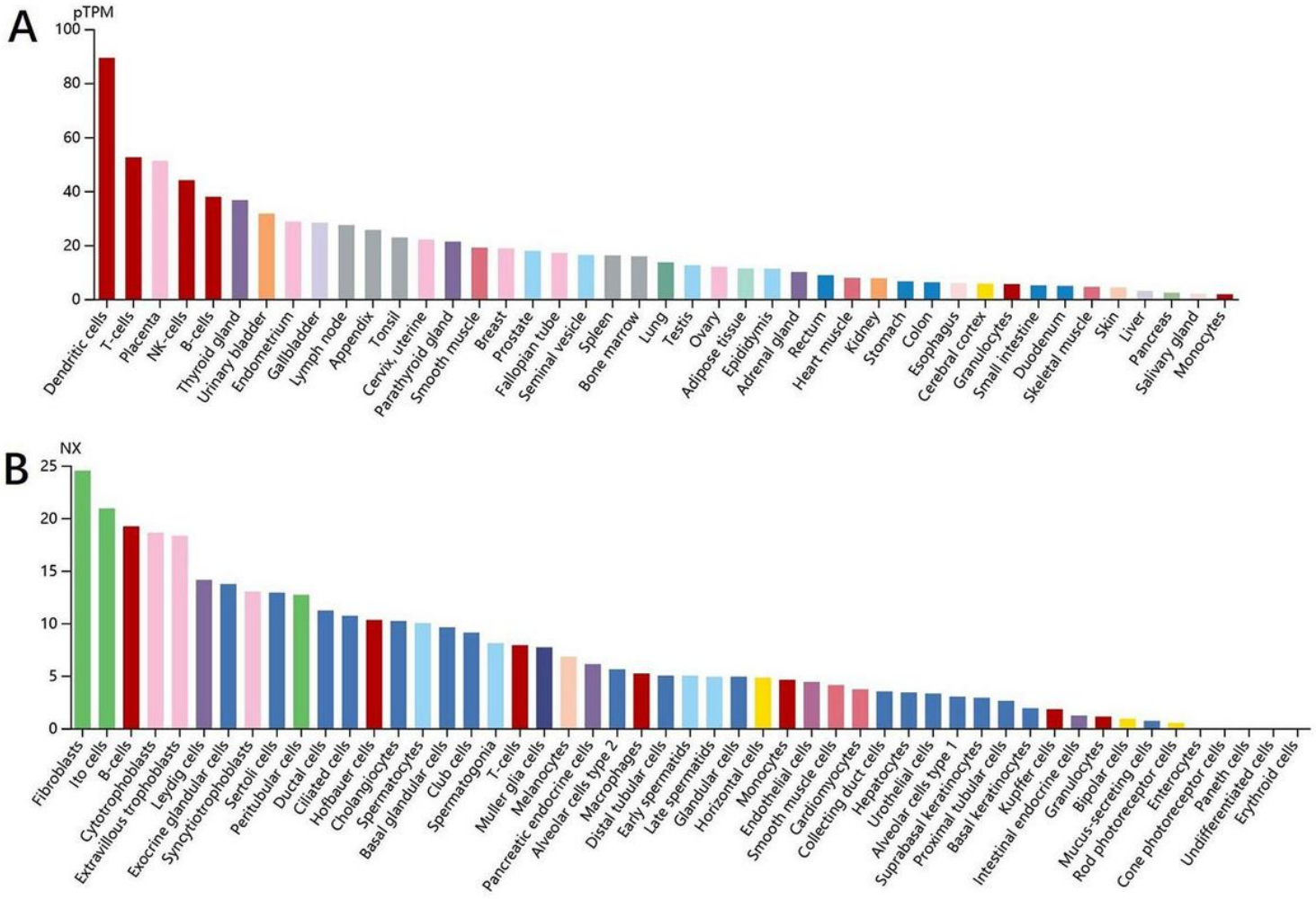

Figure 1

Expression levels and distribution of GPX7 mRNA in human normal tissues and cell lines. (A) Expression levels and distribution of GPX7 mRNA in human normal tissues. Log2 (TPM+1) was applied for log-scale. (B) Expression levels and distribution of GPX7 mRNA in human cell lines. NX (Normalized expression), calculated for each gene in each sample, was used to estimate the level of mRNA expression.

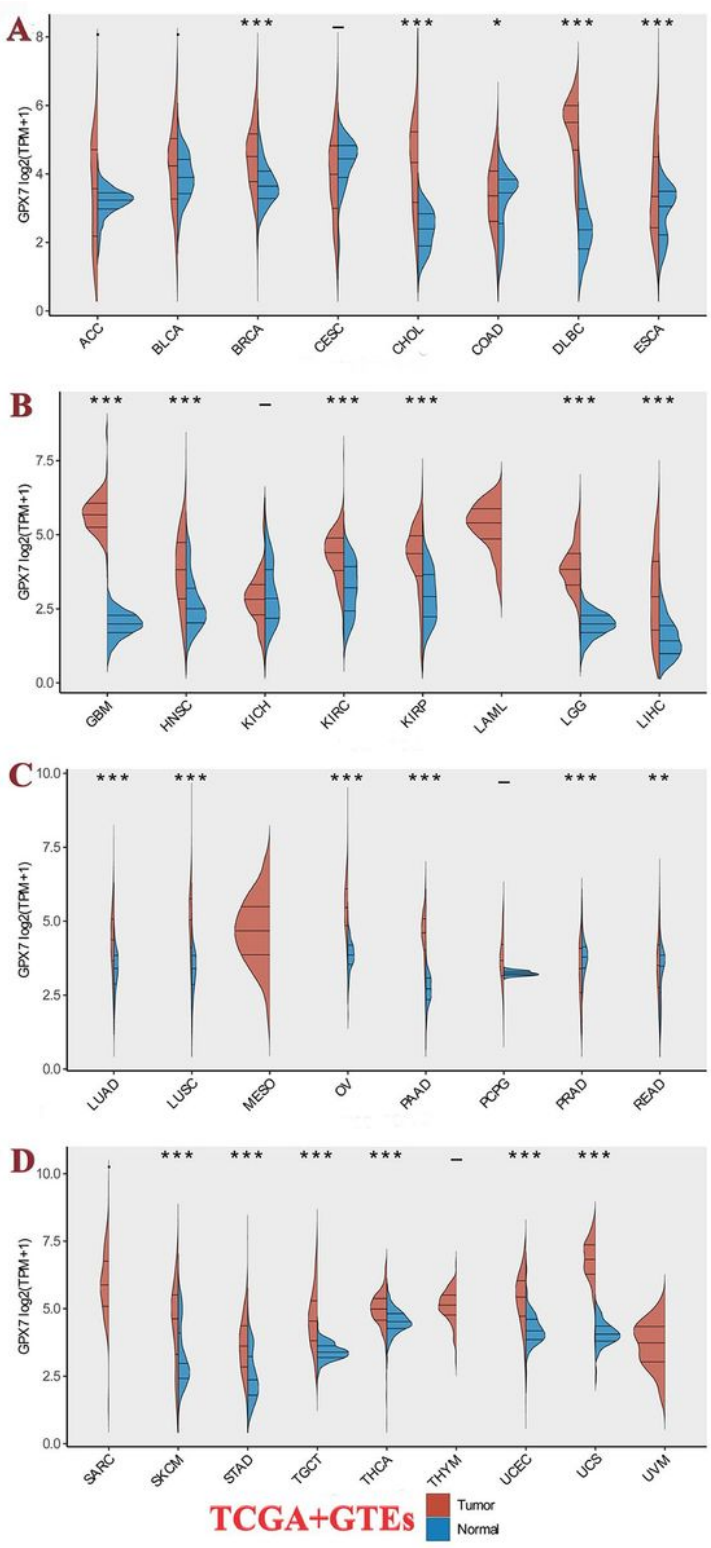

Figure 2

Expression levels of GPX7 mRNA in human tumor tissues and normal tissues.

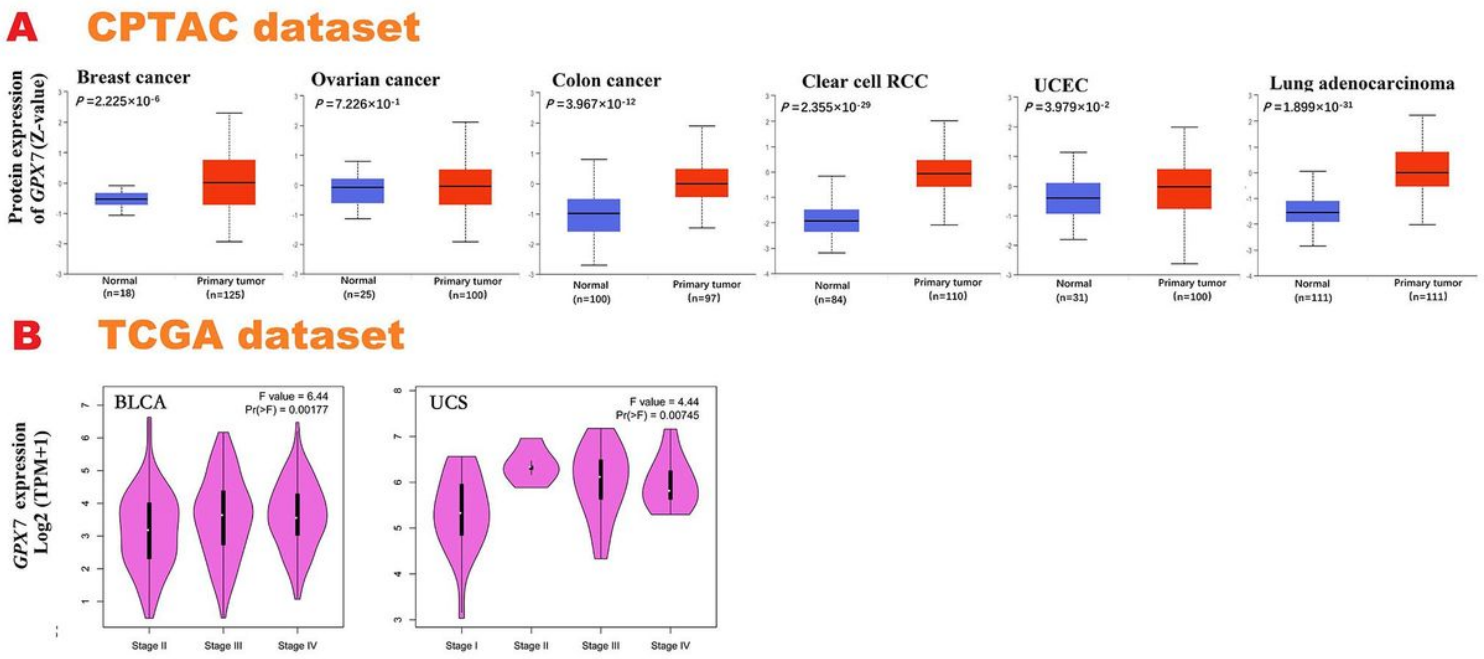

Figure 3

Expression levels of GPX7 protein in the normal tissues and primary tumors tissues. (A) Expression levels of GPX7 protein in the normal tissues and primary tissues of six tumors. (B) Expression levels of GPX7 protein in different pathological stages of BLCA and UCS.

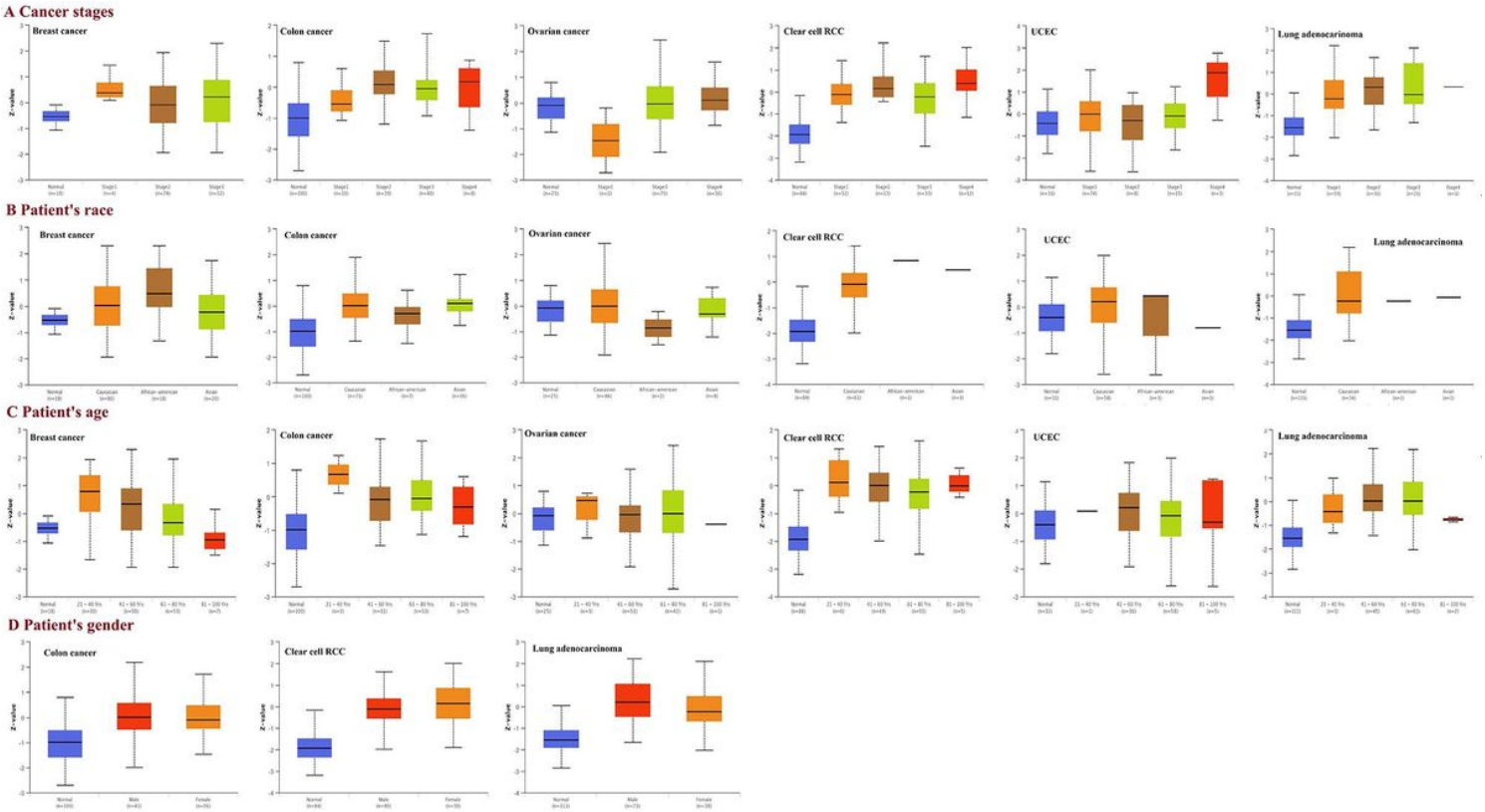

Figure 4

The relationship between GPX7 protein expression and clinicopathological parameters. (A) The relationship between GPX7 protein expression and cancer stage. (B) The relationship between GPX7 protein expression and patients' race. (C) The relationship between GPX7 protein expression and patients' age. (D) The relationship between GPX7 protein expression and patients' gender.

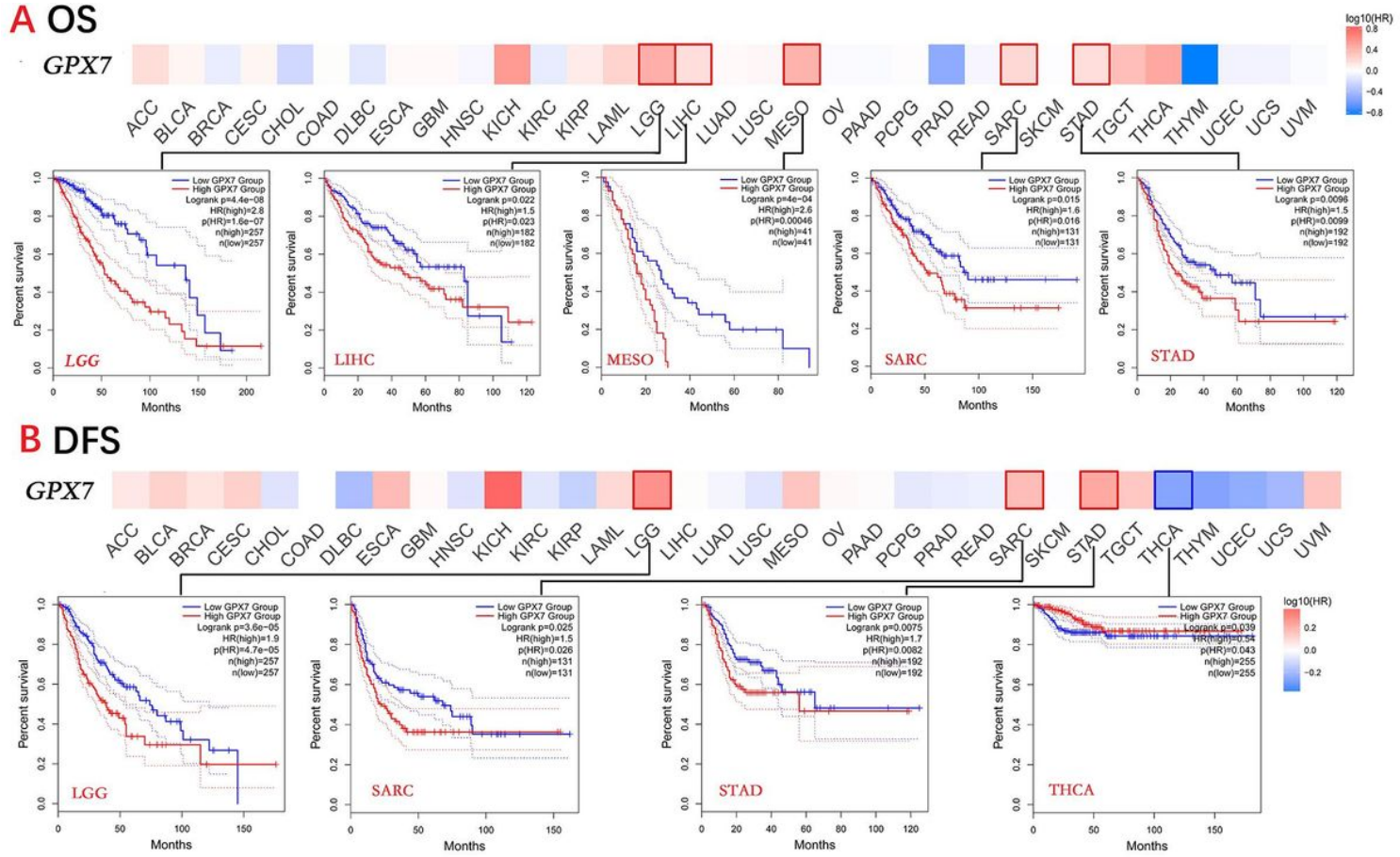

Figure 5

Correlation between GPX7 expression and survival prognosis of cancers. (A) Survival map between GPX7 gene expression and OS was established using the GEPIA2 tool. Kaplan-Meier curves with positive results were presented. (B) Survival map between GPX7 gene expression and DFS was established using the GEPIA2 tool. The Kaplan-Meier curves with positive results were presented.

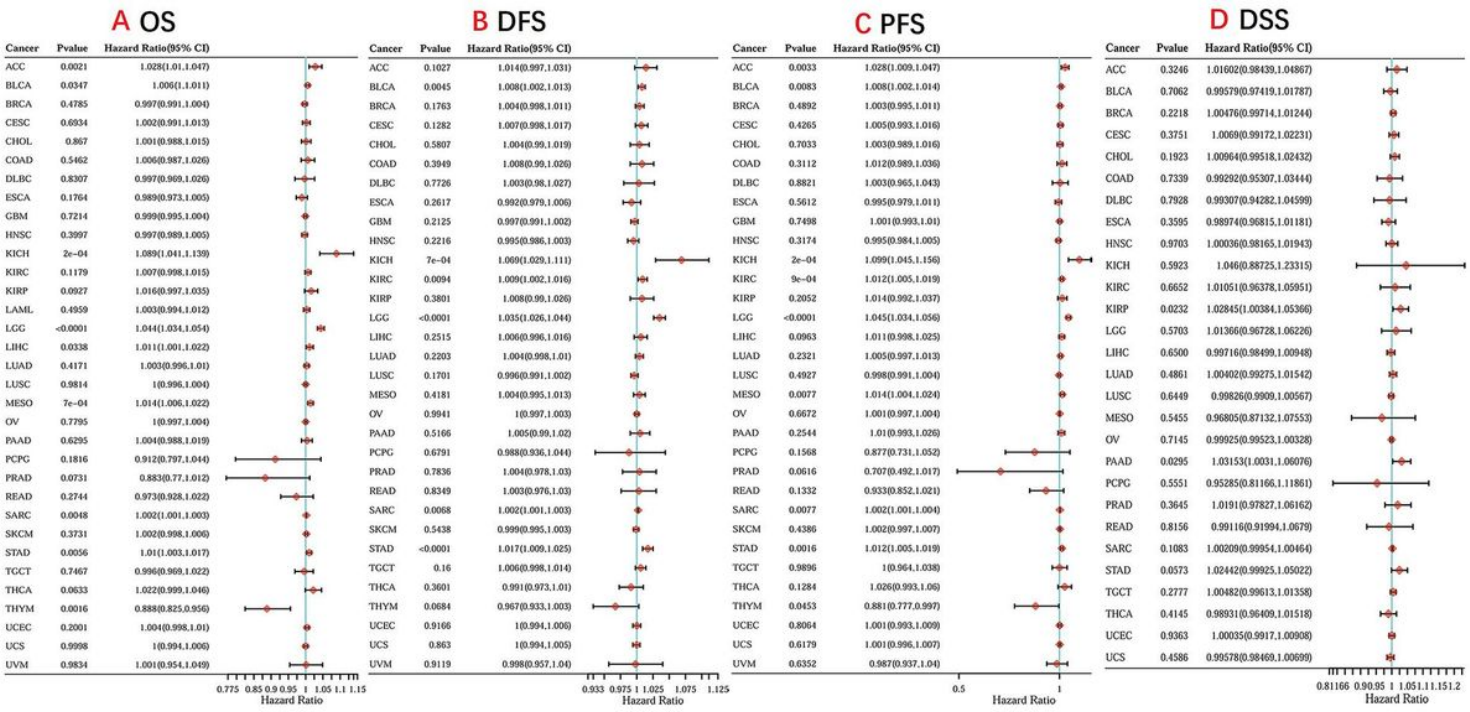

Figure 6

Forest plot for GPX7 association with tumor survival from TCGA database. (A) Forest plot of GPX7 associated with OS in TCGA tumors. (B) Forest plot of GPX7 associated with DFS in TCGA tumors. (C) Forest plot of GPX7 associated with PFS in TCGA tumors. (D) Forest plot of GPX7 associated with DSS in TCGA tumors.

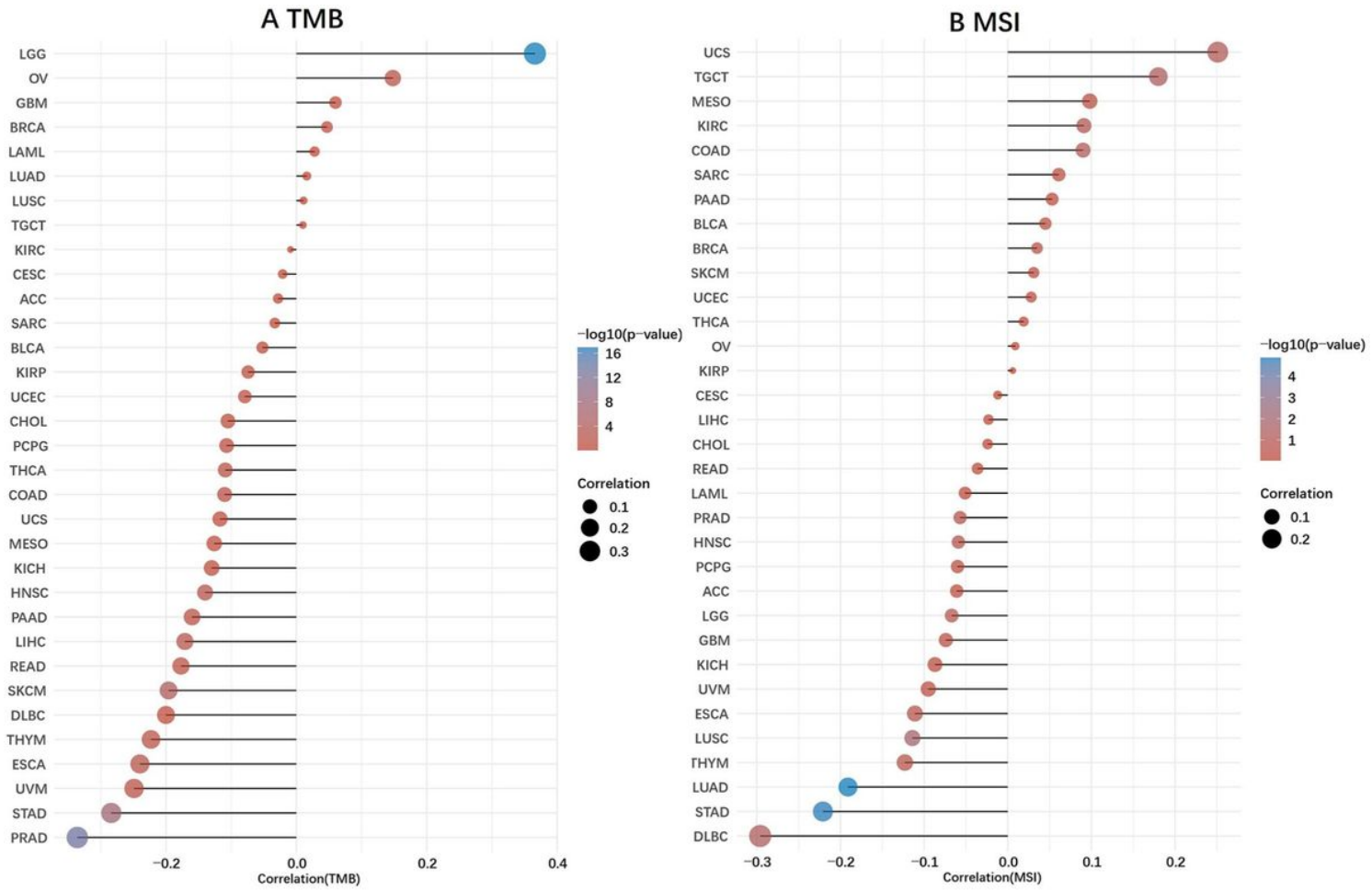

Figure 7

Relationship between GPX7 mRNA expression and TMB/ MSI in TCGA tumors. (A) Correlation between GPX7 expression and TMB. (B) Correlation between GPX7 expression and MSI.

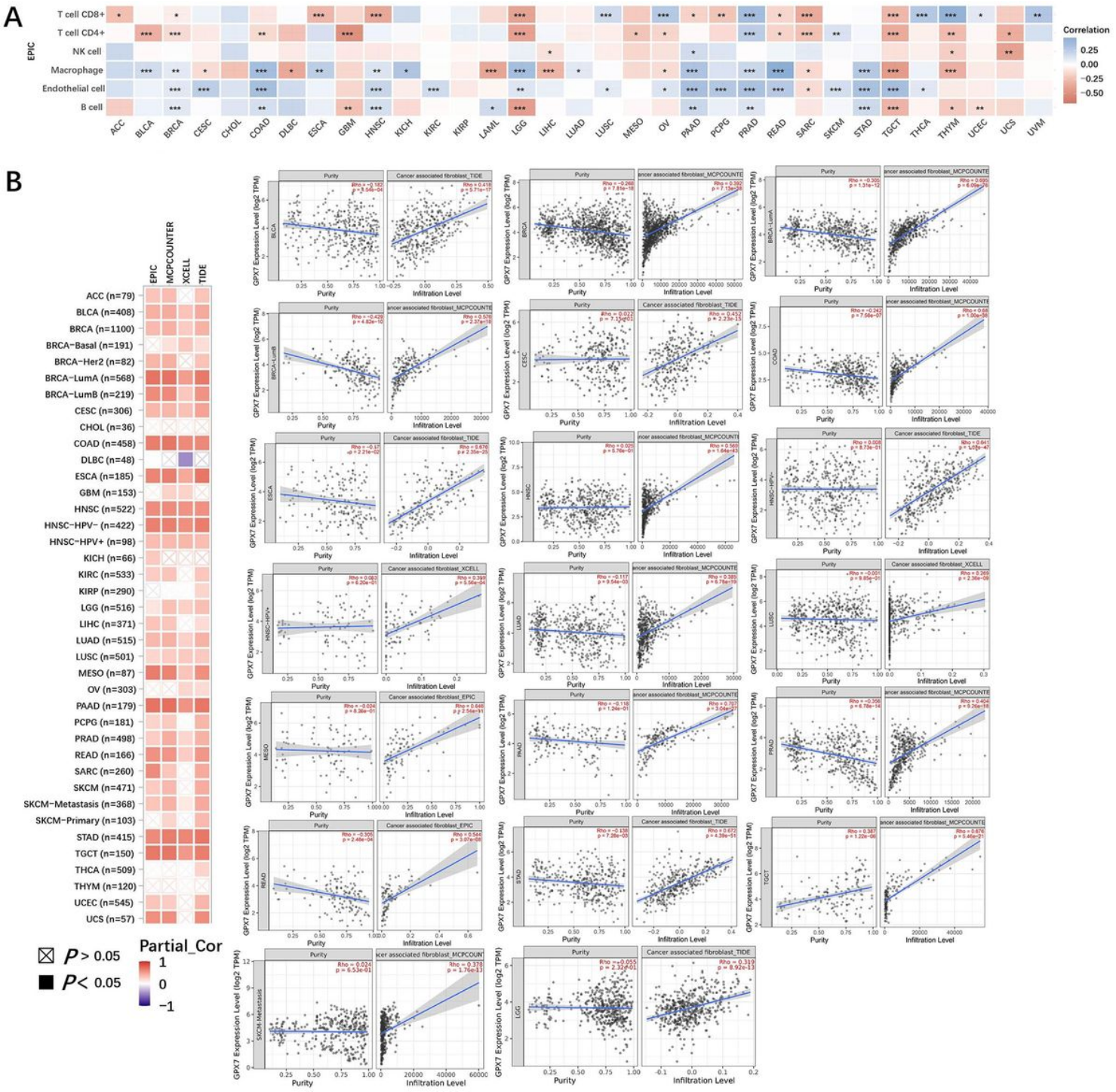

Figure 8

Correlation between GPX7 expression and immune cells infiltration. (A) Correlation between GPX7 expression and infiltration levels of six important immune cells, as determined by the EPIC algorithm. (B) Correlation between GPX7 expression and immune infiltration of CAFs, as determined using four algorithms: EPIC, MCPCOUNTER, XCELL, TIDE.

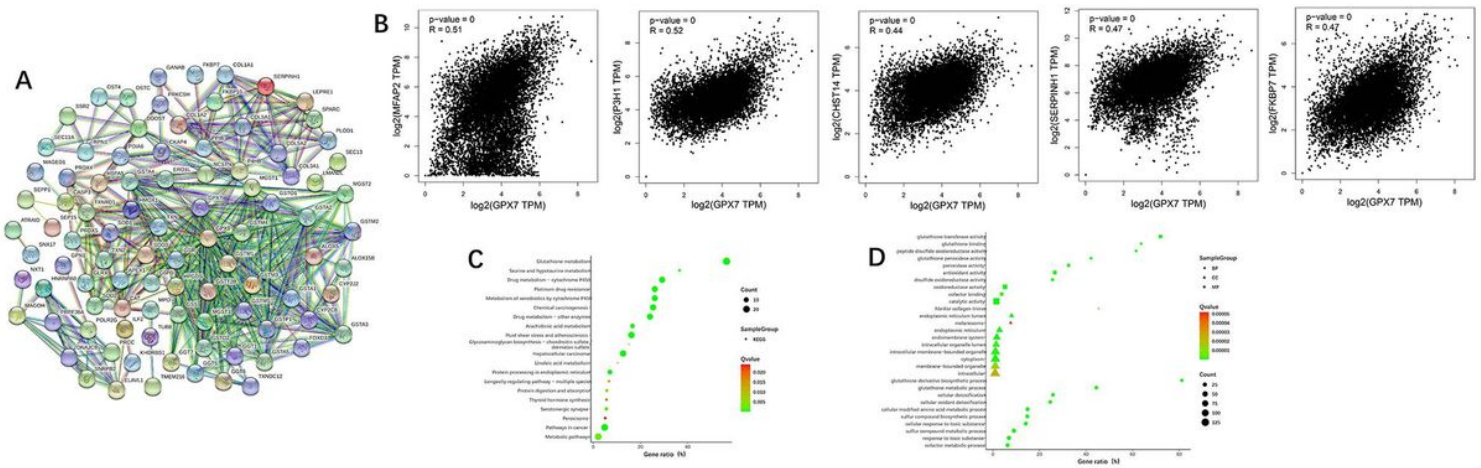

Figure 9

Enrichment analysis of GPX7-related genes. (A) PPI network of GPX7-related gene. The top 100 and the top 50 targeted genes related to GPX7 were obtained by GEPIA2 and STRING, respectively. (B) Scatter plots for the expressions of the top 5 target genes MFAP2, P3H1, CHST14, SERPINH1, FKBP7 and GPX7. (C) KEGG pathways of the top 20 genes associated with GPX7. (D) GO terms of the top 10 genes associated with GPX7, including BP, MF, and CC.

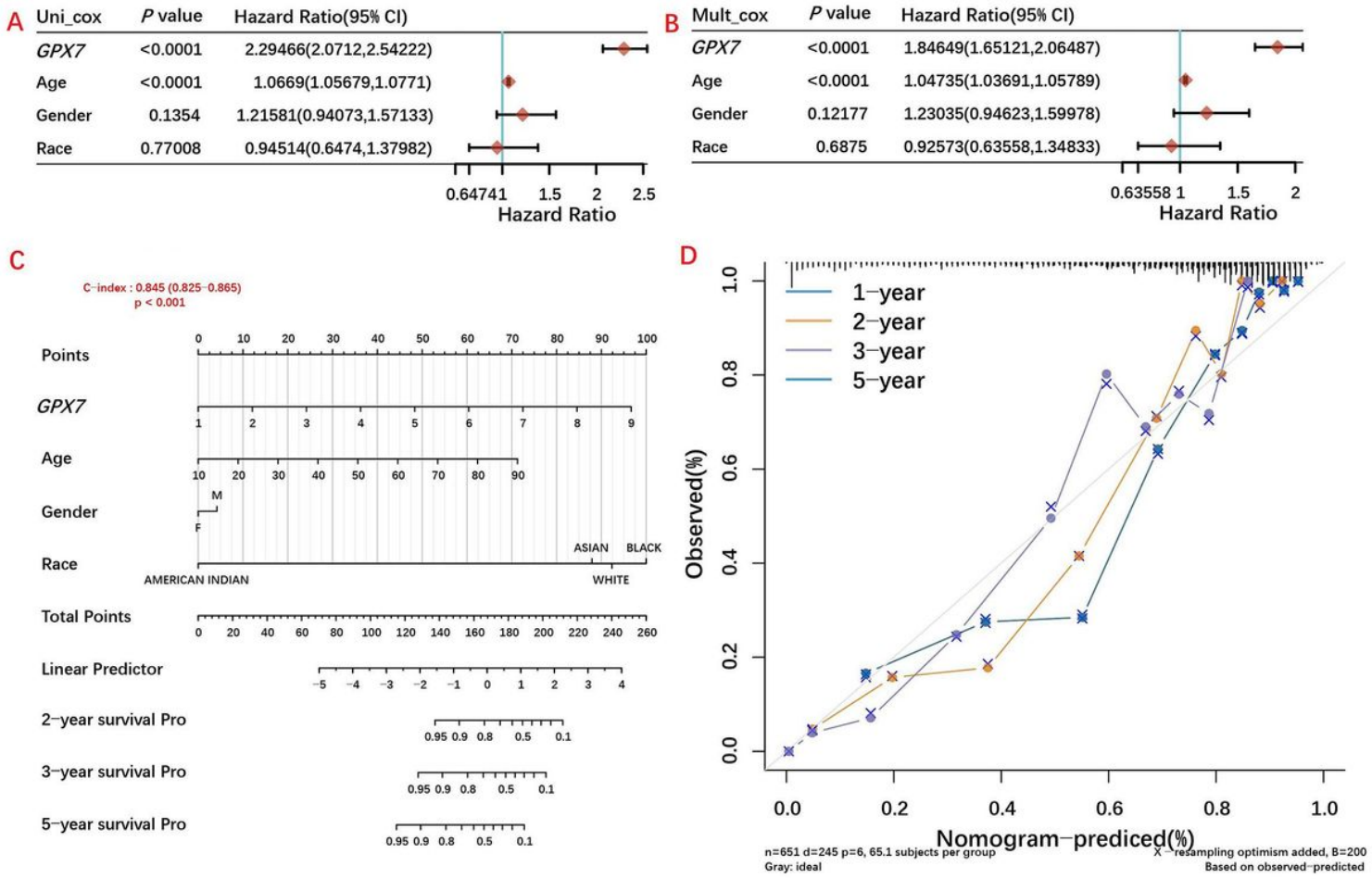

Figure 10

Construction and validation of the prognostic nomogram for LGG. (A) Univariate Cox proportional hazards regression analysis of clinical parameters with OS of LGG patients. (B) Multivariate Cox proportional hazards regression analysis of clinical parameters with OS of LGG patients. (C) Prognostic nomogram to predict 2-,3- and 5-year OS of LGG patients. (D) Calibration curves were used to calibrate the OS predictive ability the nomogram.